J. Fluid Mech. (1969), *vol.* 37, *part* 3, *pp.* 479–489
Printed in Great Britain

Jets from two-dimensional symmetric nozzles of arbitrary shape

By BRUCE E. LAROCK
University of California, Davis

(Received 4 September 1968)

A unified approach to the problem of jet efflux from symmetrical channels of finite width and possessing a general curvilinear nozzle shape is presented. The nozzle may be composed of polygonal and/or curved-arc segments. Precise nozzle shapes cannot be initially prescribed, however. The solution is based on the combined use of conformal mapping and the Riemann–Hilbert solution to a mixed boundary-value problem. The selection of an appropriate curvature function is described; examples show possible applications.

1. Introduction

The potential flow of a fluid jet from two-dimensional vessels of various shapes has attracted the attention of hydrodynamicists for over a century. As new analytical approaches are devised we come progressively closer to the solution of the general problem. As one more step in this direction the present paper presents a unified approach to the problem of jet efflux from symmetrical channels of finite width and possessing a general curvilinear nozzle shape. The nozzle may be composed of polygonal and/or curved-arc segments.

Robertson (1965), Gilbarg (1960), and Birkhoff & Zarantonello (1957) each survey most of the analytical advances in technique since the introduction of the free streamline concept by Helmholtz (1868) that has made past progress possible. Historically the development of solutions for jet efflux from polygonal nozzles has preceded the development of solutions applicable to curvilinar nozzles. Flows from infinite reservoirs were first studied; the efflux past planar nozzles from channels of finite width came next. During this period the techniques of free streamline analysis, that is, the analysis of the class of mixed boundary-value problems encountered in this work, were refined and to a degree systematized. The complex potential and the hodograph or logarithmic hodograph planes were constructed. These planes were related to one another by conformally mapping them to a common parametric plane, usually the half-plane, unit circle or the semicircle; the Schwarz–Christoffel transformation came to play an increasingly important role here.

Solutions for the jet efflux from nozzles with curved boundaries were more difficult to construct. In part this difficulty occurred because the hodograph plane could not be directly constructed for these cases, although at least one investigator

(see Milne-Thomson 1968, p. 312) has initially prescribed the shape of a logarithmic hodograph plane and achieved an interesting result. The first solutions were given by Cisotti (1908) as an extension of the work of Levi-Civita (1907). For a given curve this work involves a polynomial series expansion, with initially unknown coefficients, in powers of a parametric variable. In this connexion Villat (1911) derived an integro-differential equation, the solution of which would give the coefficients of the series. However, the direct solution of a problem via these inverse methods was difficult.

Of greater relevance to the present work are two newer publications. In a recent English translation Sedov (1965) presents a solution for an unbounded free

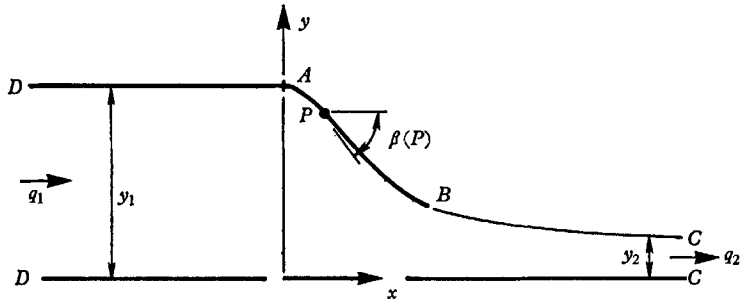

FIGURE 1. Half of symmetric nozzle, the physical plane.

streamline flow past an arbitrary number of curvilinear arcs. Also given with the solution is an integro-differential equation which governs the curvature function. The solution is based on a general solution given previously by Keldysh & Sedov (1937) for mixed boundary-value problems. Larock & Street (1968) also present a non-linear solution for a cambered body in fully cavitating flow which embodies in it a mixed boundary-value problem which is closely related to the current work.

2. General theory

We study the steady, two-dimensional, irrotational flow of an incompressible, homogeneous fluid from a symmetric nozzle of arbitrary shape. The influences of gravity, viscosity and surface tension are neglected. Figure 1 shows half of the physical plane (z plane) for this flow with the x co-ordinate chosen to coincide with the axis of symmetry. Far upstream at point D the channel is of unvarying half-width y_1 and conveys a flow at the uniform speed q_1. The y co-ordinate axis is chosen to intersect the channel wall at point A, where the curvilinear nozzle begins. Between point A and the lip of the nozzle at point B is the nozzle boundary, each point P of which may possess an arbitrary inclination $\beta(P)$, $0 < \beta < \pi$. The flow separates smoothly at point B and eventually contracts to a jet of half-width y_2 and uniform speed q_2 at point C far downstream.

In this problem we may write Bernoulli's equation as

$$p + \tfrac{1}{2}\rho q^2 = \text{constant}, \tag{1}$$

where p is the pressure, ρ is the constant fluid density, and q is the magnitude of the velocity. Also, for mass conservation

$$q_1 y_1 = q_2 y_2. \tag{2}$$

Thus, when the ratio y_1/y_2 is prescribed, unique values for q_1/q_2 and the upstream pressure are also set. Furthermore, we note in the absence of gravity that the speed q_2 prevails everywhere along the free streamline BC. In this work y_2 and q_2 are chosen as a convenient reference length and flow-speed, respectively.

In the plane of the complex potential $W = \phi + i\psi$ the image of the flow is an infinite slit, as shown in figure 2; here ϕ is the velocity potential and ψ is the stream function. The streamline $\psi = 0$ is chosen to coincide with the free streamline. The W plane and the physical z plane are related by

$$\zeta = \frac{1}{q_2}\frac{dW}{dz} = \frac{q}{q_2}e^{-i\theta}, \tag{3}$$

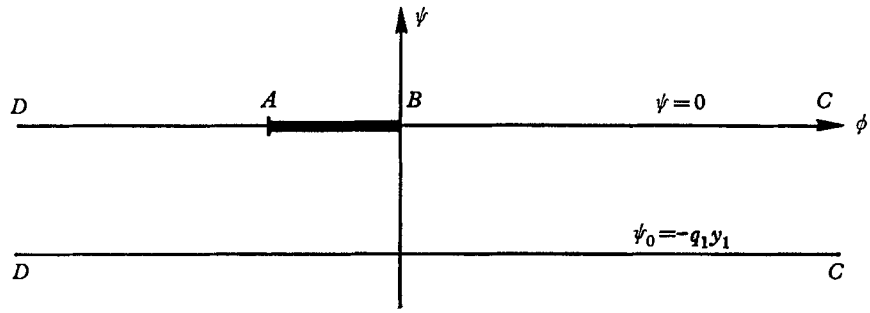

FIGURE 2. Plane of the complex potential $W = \phi + i\psi$.

where ζ is the normalized complex velocity, and θ is the argument of the velocity. In terms of the more convenient variable

$$\omega = \ln \zeta = \ln (q/q_2) + i(-\theta), \tag{4}$$

(3) can be rearranged to give z in the form

$$z = \frac{1}{q_2}\int e^{-\omega(t)}\frac{dW}{dt}dt, \tag{5}$$

where ω and W are each assumed to be expressible as functions of the same variable of integration. Our method of solution is dedicated to this goal.

The solution technique consists of two basic steps: (*a*) constructing conformal mappings between the physical and complex potential planes and a parametric half-plane, called the t plane, and (*b*) solving in this half-plane a well-posed mixed boundary-value problem for $\omega(t)$. The solution requires an appropriate prescription of the curvature function $\beta(t)$ in the half-plane. We should remark that a hodograph or logarithmic hodograph plane is never directly used in the solution of the problem, so the fact that its shape is initially unknown is of no consequence. Complex variable theory is used, but the final results are easily expressed as real quadratures that can be evaluated quickly on a high-speed digital computer.

First we map the W plane to the t plane, as in figure 3, with the boundaries of the flow domain mapped onto the real line. The curvilinear nozzle boundary AB and the free streamline BC are mapped onto finite line segments by the following chosen point correspondence for points B, C, and D, which assures uniqueness of the mapping (Churchill 1960):

$$\left.\begin{aligned} &B\colon W = 0, && t = 0,\\ &C\colon W \to +\infty, && t = -1,\\ &D\colon W \to -\infty, && t \to \infty. \end{aligned}\right\} \tag{6}$$

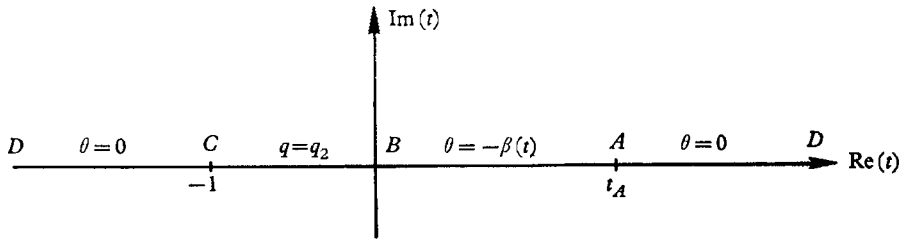

FIGURE 3. The parametric t-plane.

By requiring that $\mathrm{Im}\,(W) = -\psi_0 = -q_2 y_2$ for real $t \leqslant -1$, the scale constant of the mapping is evaluated; the mapping is thus

$$W(t) = -\frac{q_2 y_2}{\pi} \ln (1+t), \tag{7}$$

which allows us to write (5) in normalized form as

$$\frac{z}{y_2} = \frac{x+iy}{y_2} = -\frac{1}{\pi}\int e^{-\omega(t)} \frac{dt}{1+t}. \tag{8}$$

Assuming that a suitable nozzle shape $\beta(t)$ has been selected, we now note that either the real or imaginary part of $\omega(t)$ is known on the entire real line, as shown in figure 3; specifically

$$\left.\begin{aligned} &\mathrm{Im}\,(\omega) = 0, && -\infty < t < -1,\\ &\mathrm{Re}\,(\omega) = 0, && -1 < t < 0,\\ &\mathrm{Im}\,(\omega) = \beta(t), && 0 < t < t_A,\\ &\mathrm{Im}\,(\omega) = 0, && t_A < t < \infty. \end{aligned}\right\} \tag{9}$$

This boundary-value specification is easily convertible into the Riemann–Hilbert problem itself, the solution of which is well known (Song 1963; Larock & Street 1965). In fact, the approach is also similar to that outlined by Sedov (1965).

Introducing a solution $H(t)$ to the homogeneous analogue of the problem posed in (9) as

$$H(t) = [t(1+t)]^{\frac{1}{2}}, \tag{10}$$

it can be shown (Larock 1969) that a solution for $\omega(t)$, valid in the entire half-plane $\mathrm{Im}\,(t) \geqslant 0$, is

$$\omega(t) = H(t)\, Q(t), \tag{11}$$

with the quotient function

$$Q(t) = \frac{1}{\pi}\int_{-\infty}^{\infty} \frac{\mathrm{Im}\,[Q(\eta)]\,d\eta}{\eta - t}, \tag{12}$$

since $\mathrm{Im}\,[Q(t)] = \mathrm{Im}\,[\omega(t)/H(t)]$ is known. In general it is possible to add a series $\Sigma A_j t^j$ to (12). This problem requires $A_j = 0$ for all j, however, because of the dual requirements that the flow separate smoothly at B and move with speed q_1 at D. Therefore

$$\omega(t) = \frac{1}{\pi} H(t) \int_0^{t_A} \frac{\beta(\eta)\,d\eta}{(\eta - t)\,[\eta(1+\eta)]^{\frac{1}{2}}}. \tag{13}$$

The analytical behaviour of $\omega(t)$ is more fully displayed in the example to follow.

The foregoing procedure has introduced an unknown constant t_A into the solution. It is determined by requiring at point D, where $t \to \infty$, that

$$\omega_D = \ln(q_1/q_2) = -\ln(y_1/y_2) = -\frac{1}{\pi}\int_0^{t_A} \frac{\beta(\eta)\,d\eta}{[\eta(1+\eta)]^{\frac{1}{2}}}. \tag{14}$$

Now $\omega(t)$ is a fully known quantity, and the precise physical-plane configuration can be computed directly from (8).

Finally, the local pressure coefficient, defined as

$$C_p = \frac{p}{\frac{1}{2}\rho q_2^2}, \tag{15}$$

may also be of interest. By using (1) and (4), we quickly find C_p is directly expressible in terms of ω and its conjugate $\overline{\omega}$ by the relation

$$C_p = 1 - \exp[\omega + \overline{\omega}], \tag{16}$$

for any point in the flow.

3. The curvature function $\beta(t)$

Ideally we would prescribe the local nozzle inclination $\beta(z)$ at each point on the nozzle boundary so the shape of the nozzle is known *a priori*. Due to the nonlinear nature of the current solution, however, this is not directly possible since here β must be initially prescribed as a function of t, not z. Nevertheless, great freedom is still possible in selecting the form of $\beta(t)$ so that shapes of physical interest result, and yet $\omega(t)$ can still be evaluated analytically.

Consider, for example, a piecewise continuous, nth degree polynomial representation for β

$$\beta(t) = \sum_{i=1}^{n} a_i t^i. \tag{17}$$

The coefficients a_i can be chosen so that $\beta(t)$ will assume a specified value β_k at each particular juncture point t_J and also at the end points $t = 0$ and $t = t_A$. If β is to change discontinuously (jump) at t_J, then both $\beta(t_J^-)$ and $\beta(t_J^+)$ are initially prescribed.

To increase the descriptive capabilities of the curvature function, we may increase the degree of the polynomial and/or increase the number of intermediate points t_J. Due to the identity

$$\frac{\eta^n}{\eta - t} = \frac{t^n}{\eta - t} + \sum_{i=1}^{n} \eta^{n-i} t^{i-1} \quad (n = 1, 2, 3, \ldots), \tag{18}$$

(13) and (14) will involve integrals only of the forms

$$\int \frac{d\eta}{(\eta - t)[\eta(1+\eta)]^{\frac{1}{2}}} \quad \text{and} \quad \int \frac{\eta^i d\eta}{[\eta(1+\eta)]^{\frac{1}{2}}} \quad (0 \leqslant i \leqslant (n-1)),$$

regardless of the degree of the chosen polynomial in (17). On the other hand, the selection of m intermediate points t_J requires us to evaluate the integrals in (13) and (14) separately over the intervals $(0, t_{J1})$, (t_{J1}, t_{J2}), ..., (t_{Jm}, t_A), rather than integrating directly over the range $(0, t_A)$. No conceptual difficulties are encountered here, but the acquisition of additional flexibility in $\beta(t)$ requires us to manipulate bulkier expressions for $\omega(t)$.

In practice, rather simple curvature functions can be used to generate a wide variety of interesting and practical nozzle shapes which are worthy of study, as the following example will illustrate. We should remember, however, that the model is constrained to allow separation only at point B. A curvature relation which presents an obtuse corner to the oncoming flow along AB will therefore produce a locally infinite velocity at that corner. Although this is unrealistic, in the real case either the local influence of viscosity would prevent that occurrence or the flow would separate at that point, which should then be labelled point B for this theory.

4. Example and solution

Let us consider a curvature function having one juncture point t_J, $0 < t_J < t_A$, and four prescribed local inclinations β_k, $k = 1, \ldots, 4$. We require at

$$\left.\begin{aligned} t &= 0, & \beta(0) &= \beta_1; \\ t &= t_J^-, & \beta(t_J^-) &= \beta_2; \\ t &= t_J^+, & \beta(t_J^+) &= \beta_3; \\ t &= t_A, & \beta(t_A) &= \beta_4. \end{aligned}\right\} \tag{19}$$

Thus $\beta(t)$ possesses a possible jump discontinuity at t_J and so, in general, is piecewise continuous. We shall prescribe the four values β_k and assume a linear variation for $\beta(t)$ over the intervals $(0, t_J)$ and (t_J, t_A). Consequently we have

$$\left.\begin{aligned} \beta(t) &= \frac{1}{t_J}[(\beta_2 - \beta_1)t + \beta_1 t_J] && (0 \leqslant t \leqslant t_J^-), \\ \beta(t) &= \frac{1}{t_A - t_J}[(\beta_4 - \beta_3)t + \beta_3 t_A - \beta_4 t_J] && (t_J^+ \leqslant t \leqslant t_A). \end{aligned}\right\} \tag{20}$$

In this case it is convenient to specify the ratio $\lambda = t_J/t_A$ in addition to the β_k and the ratio y_1/y_2.

The parameter t_A is found from (14), which now takes the form

$$\begin{aligned} \pi \ln\left(\frac{y_1}{y_2}\right) = {} & \frac{\beta_2 - \beta_1}{t_J}[t_J(1+t_J)]^{\frac{1}{2}} + \left[\beta_1 - \frac{1}{2t_J}(\beta_2 - \beta_1)\right] \ln\left(2t_J + 1 + 2[t_J(1+t_J)]^{\frac{1}{2}}\right) \\ & + \frac{\beta_4 - \beta_3}{t_A - t_J}\left([t_A(1+t_A)]^{\frac{1}{2}} - [t_J(1+t_J)]^{\frac{1}{2}}\right) \\ & + \frac{1}{t_A - t_J}[\beta_3 t_A - \beta_4 t_J - \tfrac{1}{2}(\beta_4 - \beta_3)] \ln\left[\frac{2t_A + 1 + 2[t_A(1+t_A)]^{\frac{1}{2}}}{2t_J + 1 + 2[t_J(1+t_J)]^{\frac{1}{2}}}\right]. \end{aligned} \tag{21}$$

A simple successive-approximation procedure will enable a digital computer to find t_A very quickly from this equation.

In this case expression (13) for $\omega(t)$ becomes

$$\pi\frac{\omega(t)}{H(t)} = \frac{1}{t_J}(\beta_2-\beta_1)\int_0^{t_J}\frac{d\eta}{[\eta(1+\eta)]^{\frac{1}{2}}} + \frac{1}{t_A-t_J}(\beta_4-\beta_3)\int_{t_J}^{t_A}\frac{d\eta}{[\eta(1+\eta)]^{\frac{1}{2}}}$$
$$+\frac{1}{t_J}[(\beta_2-\beta_1)t+\beta_1 t_J]\int_0^{t_J}\frac{d\eta}{(\eta-t)[\eta(1+\eta)]^{\frac{1}{2}}}$$
$$+\frac{1}{t_A-t_J}[(\beta_4-\beta_3)t+\beta_3 t_A-\beta_4 t_J)]\int_{t_J}^{t_A}\frac{d\eta}{(\eta-t)[\eta(1+\eta)]^{\frac{1}{2}}} \tag{22}$$

when modified according to (18). By defining the quantities

$$M_1(t) = \left\{\frac{1}{\pi}\left(\frac{\beta_2-\beta_1}{t_J}\right)\ln[2t_J+1+2[t_J(1+t_J)]^{\frac{1}{2}}]\right.$$
$$\left.+\frac{1}{\pi}\left(\frac{\beta_4-\beta_3}{t_A-t_J}\right)\ln\left[\frac{2t_A+1+2[t_A(1+t_A)]^{\frac{1}{2}}}{2t_J+1+2[t_J(1+t_J)]^{\frac{1}{2}}}\right]\right\}[t(1+t)]^{\frac{1}{2}}, \tag{23a}$$

$$M_2(t) = -\frac{1}{\pi}\left[(\beta_2-\beta_1)\frac{t}{t_J}+\beta_1\right]\ln\left|\frac{2[tt_J(1+t)(1+t_J)]^{\frac{1}{2}}+t+t_J+2tt_J}{t-t_J}\right|, \tag{23b}$$

$$M_3(t) = -\frac{1}{\pi}\left(\frac{1}{t_A-t_J}\right)[(\beta_4-\beta_3)t+\beta_3 t_A-\beta_4 t_J]$$
$$\times\ln\left|\left(\frac{2[tt_A(1+t)(1+t_A)]^{\frac{1}{2}}+t+t_A+2tt_A}{2[tt_J(1+t)(1+t_J)]^{\frac{1}{2}}+t+t_J+2tt_J}\right)\left(\frac{t_J-t}{t_A-t}\right)\right|, \tag{23c}$$

and

$$M(t) = \sum_{j=1}^{3} M_j(t), \tag{23d}$$

for $0 < t < t_A$, we obtain on the nozzle boundary

$$\omega(t) = M(t)+i\beta(t). \tag{24}$$

By substitution into (8) we obtain two parametric expressions for the co-ordinates of the nozzle boundary:

$$\frac{x(t)-x_0}{y_2} = -\frac{1}{\pi}\int_{t_0}^{t<t_0}\frac{\exp[-M(\eta)]\cos\beta(\eta)\,d\eta}{1+\eta}, \tag{25a}$$

$$\frac{y(t)-y_0}{y_2} = \frac{1}{\pi}\int_{t_0}^{t<t_0}\frac{\exp[-M(\eta)]\sin\beta(\eta)\,d\eta}{1+\eta}. \tag{25b}$$

For integration from point A towards point B we select $t_0 = t_A$, and for the chosen co-ordinate system $x_0 = 0$ and $y_0 = y_1$. Then along the nozzle boundary the local pressure coefficient is easily calculated to be

$$C_p = 1-e^{2M(t)} \quad (0 < t < t_A). \tag{26}$$

The expression for $\omega(t)$ on the free streamline is entirely imaginary, since there $q = q_2$ everywhere on the fluid surface. We shall write

$$\omega(t) = iB(t) \quad (-1 < t < 0), \tag{27}$$

with
$$B(t) = \sum_{j=1}^{3} B_j(t), \tag{28a}$$

$$B_1(t) = \frac{1}{\pi}[-t(1+t)]^{\frac{1}{2}}\left\{\frac{1}{t_J}(\beta_2-\beta_1)\ln[2t_J+1+2[t_J(1+t_J)]^{\frac{1}{2}}]\right.$$
$$\left.+\frac{1}{t_A-t_J}(\beta_4-\beta_3)\ln\left[\frac{2t_A+1+2[t_A(1+t_A)]^{\frac{1}{2}}}{2t_J+1+2[t_J(1+t_J)]^{\frac{1}{2}}}\right]\right\}, \tag{28b}$$

$$B_2(t) = \frac{1}{\pi}[(\beta_2-\beta_1)\frac{t}{t_J}+\beta_1]\left\{\sin^{-1}\left[1+2t+\frac{2t(1+t)}{t_J-t}\right]+\frac{\pi}{2}\right\}, \tag{28c}$$

and
$$B_3(t) = \frac{1}{\pi}\left(\frac{1}{t_A-t_J}\right)[(\beta_4-\beta_3)t+\beta_3 t_A-\beta_4 t_J]\left\{\sin^{-1}\left[1+2t+\frac{2t(1+t)}{t_A-t}\right]\right.$$
$$\left.-\sin^{-1}\left[1+2t+\frac{2t(1+t)}{t_J-t}\right]\right\}. \tag{28d}$$

Again from (8) the free streamline co-ordinates are given parametrically by

$$\frac{x(t)-x_0}{y_2} = -\frac{1}{\pi}\int_{t_0}^{t<t_0}\frac{\cos B(\eta)\,d\eta}{1+\eta}, \tag{29a}$$

and
$$\frac{y(t)-y_0}{y_2} = \frac{1}{\pi}\int_{t_0}^{t<t_0}\frac{\sin B(\eta)\,d\eta}{1+\eta}. \tag{29b}$$

By beginning the integrations from the nozzle tip, point B, we have

$$t_0 = 0, \quad x_0 = x_B = x(0) \quad \text{and} \quad y_0 = y_B = y(0).$$

5. Results

Figures 4 to 6 present several computed nozzle shapes together with listings of the pertinent parameters for each nozzle. Here $b = y_B$ is the nozzle half-width, and $C_c = y_2/b$ is the contraction coefficient for the nozzle.

As figures 4 to 6 show, even the relatively simple curvature function selected for the preceding examples is capable of producing a number of interesting and useful nozzle shapes. Strictly speaking, the solution procedure is inverse in the sense that the physical situation under study is not initially prescribed in the physical plane itself. In practice, this feature is merely an inconvenience. Only a modest amount of experience in selecting input parameters is needed before a given physical case (assuming the physical case is of a class which is representable by the chosen curvature function) can be reproduced with reasonable precision. To a large extent this is true because the chosen local nozzle inclinations β_k have direct physical meaning rather than being purely abstract parameters, and for this reason it is felt that an analogue of Villat's and Sedov's integro-differential equations for curvature would actually prove to be an analytical hindrance rather than an aid to this study.

Figure 4 shows two similar nozzles for $y_1/y_2 = 6$ and equal local inclinations $\beta = 70°$ at the nozzle lip where the free streamline separates smoothly from the solid boundary. In case A the local inclination was everywhere a constant 70°.

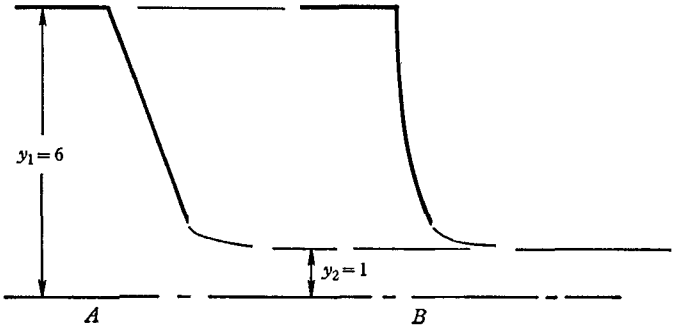

FIGURE 4. Effect of curvature for $y_1/y_2 = 6$. Planar nozzle A: $\beta_k = 70°$, $t_A = 24{\cdot}6$; $b/y_1 = 0{\cdot}2508$, $C_c = 0{\cdot}6645$. Curved nozzle B: $\beta_1 = 70°$, $\beta_2 = \beta_3 = 80°$, $\beta_4 = 90°$, $\lambda = 0{\cdot}5$, $t_A = 18{\cdot}8$; $b/y_1 = 0{\cdot}2516$, $C_c = 0{\cdot}6623$.

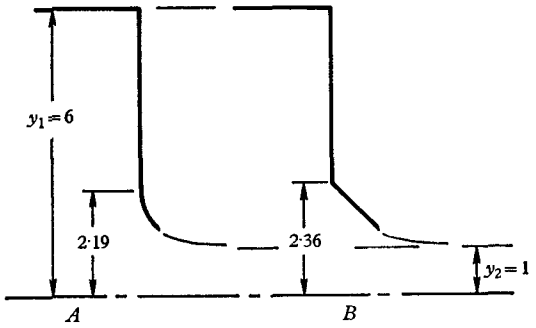

FIGURE 5. Variation of nozzle tip shape for $y_1/y_2 = 6$ and $\lambda = 0{\cdot}2$. Nozzle tip A: $\beta_1 = 45°$, $\beta_2 = \beta_3 = \beta_4 = 90°$, $t_A = 30{\cdot}2$; $b/y_1 = 0{\cdot}2301$, $C_c = 0{\cdot}7242$. Nozzle tip B: $\beta_1 = \beta_2 = 45°$, $\beta_3 = \beta_4 = 90°$, $t_A = 66{\cdot}2$; $b/y_1 = 0{\cdot}2240$, $C_c = 0{\cdot}7439$.

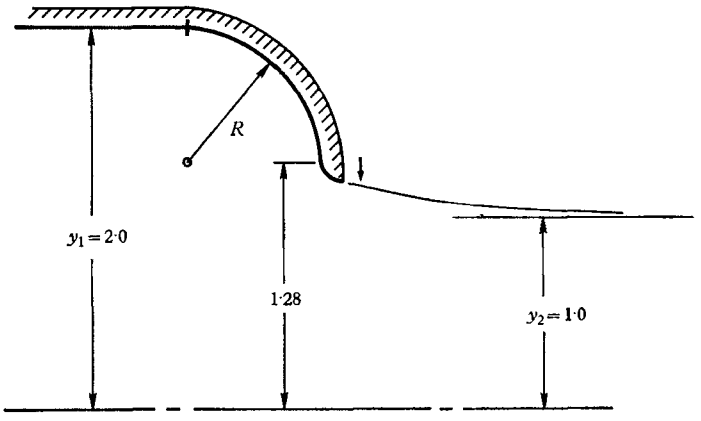

FIGURE 6. The rounded nozzle: $y_1/y_2 = 2{\cdot}0$, $\lambda = 0{\cdot}2$, $\beta_1 = \beta_4 = 0°$, $\beta_2 = \beta_3 = 90°$, $t_A = 5{\cdot}786$; $b/y_1 = 0{\cdot}5923$, $C_c = 0{\cdot}8442$.

In case B the local nozzle curvature varied linearly, as a function of t, from 70° at the lip to 90°. These data suggest that C_c is dependent primarily on the local inclination of the nozzle lip and not on the geometry away from the lip. Recently Henderson (1966, p. 206) has remarked similarly on this behaviour.

The effect of a greater local difference in boundary geometry near the lip is illustrated in figure 5. We observe that only one prescribed input parameter, β_2, was changed from case A to case B. The change in geometry changed values of b/y_1 and C_c each by approximately 2·5 per cent.

A selected linear variation for $\beta(t)$ can result in nozzle boundaries which consist of very nearly circular-arc segments; an example is shown in figure 6 where the nozzle is composed of a 90° arc of radius $R \approx 0{\cdot}70$ and a smoothly rounded exit lip. Figures 4 and 5 also show examples of this behaviour.

An interesting feature of the sample in figure 6 is the point of inflexion present on the free streamline near the nozzle lip at the location of the arrow. The calculations from which this figure was prepared show a maximum streamline inclination of 13·3° at this point. Far downstream this streamline becomes horizontal; by construction the nozzle lip inclination is $\beta_1 = 0$ degrees, and one feature of all solutions using the present method is the existence of smooth separation at the lip. The presence of the inflexion point in the free streamline is caused by the reversed curvature or inflexion in the nozzle tip shape. Birkhoff & Zarantonello (1957) discuss such free-boundary inflexions more fully.

Computational work for these examples was performed on the IBM 7044 digital computer at the Computer Center of the University of California, Davis. Three distinct factors tended to increase execution time on a numerical example. Execution time lengthened when y_1/y_2 was increased, and it also increased when low local inclinations β were assigned to large portions of a given nozzle geometry. The result of either action was to require a large t_A to satisfy (14), and thereby increase the range of integration in the quadratures (25), which parametrically describe the nozzle configuration. And, of course, execution time would increase somewhat as a result of imposing increased accuracy requirements in the evaluation of the quadratures.

The combined use of conformal mapping and the Riemann–Hilbert solution to a mixed boundary-value problem produces the theoretical solution for flow past a wide class of symmetrical nozzles of arbitrary shape from a channel of finite width. The judicious selection of an appropriate curvature function and use of a high-speed digital computer for evaluating the resulting expressions combine to make the theory usable in a practical way.

REFERENCES

Birkhoff, G. & Zarantonello, E. H. 1957 *Jets, Wakes and Cavities*. New York: Academic Press.

Churchill, R. V. 1960 *Complex Variables and Applications*, 2nd ed. New York: McGraw-Hill.

Cisotti, V. 1908 Esempio di efflusso da un recipients a serzione non rettilinea. *R.C. mat. Palermo*, **26**, 378–382.

Gilbarg, D. 1960 Jets and cavities. *Handb. Phys.* **9**, 311–445.

HELMHOLTZ, H. 1868 On the discontinuous motion of fluids. *Trans. Phil. Mag.* (4) **36**, 337–345.

HENDERSON, F. M. 1966 *Open Channel Flow.* New York: Macmillan.

KELDYSH, M. V. & SEDOV, L. I. 1937 Effective solution of some problems for harmonic functions. *Dokl. Akad. Nauk, SSSR*, **16**, 1.

LAROCK, B. E. 1969 Gravity-affected flow from planar sluice gates. *J. Hydraulics Division, Proc. Am. Soc. Civil Eng.* (to appear).

LAROCK, B. E. & STREET, R. L. 1965 A Riemann–Hilbert problem for nonlinear, fully cavitating flow. *J. Ship. Res.* **9**, 170–178.

LAROCK, B. E. & STREET, R. L. 1968 Cambered bodies in cavitating flow—a nonlinear analysis and design procedure, *J. Ship. Res.* **12**, 1–13.

LEVI-CIVITA, T. 1907 Scie e leggi di resistenza. *R. C. mat. Palermo*, **23**, 1–37.

MILNE-THOMSON, L. M. 1968 *Theoretical Hydrodynamics*, 5th ed. New York: Macmillan.

ROBERTSON, J. M. 1965 *Hydrodynamics in Theory and Application.* Englewood Cliffs, N.J.: Prentice-Hall.

SEDOV, L. I. 1965 *Two-dimensional Problems in Hydrodynamics and Aerodynamics.* New York: Wiley.

SONG, C. S. 1963 A quasi-linear and linear theory for non-separated and separated two-dimensional, incompressible, irrotational flow about lifting bodies. *University of Minnesota, Minneapolis SAF Hydraulic Lab. Tech. Paper*, B 43.

VILLAT, H. 1911 Sur la résistance des fluids. *Ann sci. ec. norm. sup. Paris*, **28**, 203–240.